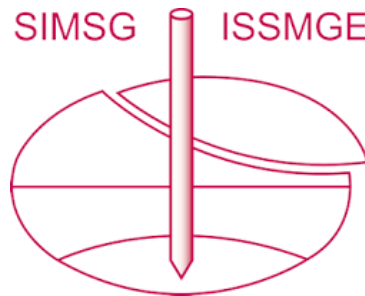


INTERNATIONAL SOCIETY FOR SOIL MECHANICS AND GEOTECHNICAL ENGINEERING



This paper was downloaded from the Online Library of the International Society for Soil Mechanics and Geotechnical Engineering (ISSMGE). The library is available here:

<https://www.issmge.org/publications/online-library>

This is an open-access database that archives thousands of papers published under the Auspices of the ISSMGE and maintained by the Innovation and Development Committee of ISSMGE.

The paper was published in the proceedings of the 7th International Conference on Earthquake Geotechnical Engineering and was edited by Francesco Silvestri, Nicola Moraci and Susanna Antonielli. The conference was held in Rome, Italy, 17 - 20 June 2019.

Evaluation of liquefaction triggering potential using the case-based reasoning method with CPT field data

J.N. Roberts & H.K. Engin

Norwegian Geotechnical Institute, Oslo, Norway

ABSTRACT: This paper presents a proof-of-concept application of the Artificial Intelligence method Case-Based Reasoning (CBR) for the prediction of liquefaction triggering potential in natural deposits. The method was applied using data from 24 case history sites in the Christchurch, New Zealand, region that experienced liquefaction during the 2010-2011 Canterbury Earthquake Sequence (CES). Liquefaction triggering at two of the 24 sites was predicted using CPT-based datasets for two separate earthquake events: the 4 September 2010 Darfield earthquake (Mw 7.1) and the 22 February 2011 Christchurch earthquake (Mw 6.2). Results from this work show that the CBR method can be used to accurately identify critical liquefiable layers and that it can produce results that are comparable to a widely-used CPT-based liquefaction triggering procedure.

1 INTRODUCTION

This paper presents a proof-of-concept application of the Case-Based Reasoning (CBR) method for predicting soil liquefaction triggering in natural deposits. CBR is an artificial intelligence (AI) method in which new problems are solved using the known solutions to old problems. While in the past 20 years there has been a steady increase in the use of AI methods in civil engineering, the majority of CBR applications are found in the area of construction management where researchers are using it for project cost and resource estimations (Kim and Shim 2014, García de Soto and Adey 2015, Zima 2015, and Lesniak and Zima 2018), construction hazard identification (Goh and Chua 2009), and construction planning and project delivery method selection (Yau and Yang 1996, Rankin et al. 1999, Ryu et al. 2007, Yoon et al. 2016). Geotechnical engineers, however, have preferred various neural network methods for applications such as predictions of liquefaction triggering, pile capacity, foundation settlement, and slope stability (Juwaied 2018). One of the main advantages over artificial neural networks (ANN) is that CBR is a fully transparent method and it allows users to follow the reasoning steps on every level. Although there are recent powerful tools for ANN (e.g. tensor flow) that allow for visualization of the network strength, the relationship between the input and output is still difficult to quantify, leaving users with a system that is more like a black box.

In this study, CBR was used to predict soil liquefaction triggering in the subsurface and to identify critical layers using raw CPT data and peak ground acceleration (PGA), much like the widely-used CPT-based liquefaction triggering methods such as Boulanger and Idriss (2016). The case history database has been populated using data from the Christchurch, New Zealand, area and from two specific earthquake events: the 4 September 2010 Darfield earthquake (Mw 7.1) and the 22 February 2011 Christchurch earthquake (Mw 6.2). The full and detailed characterization of the sites that were included in the database was originally performed by the authors of Green et al. (2014) and raw data was downloaded from the New Zealand Geotechnical Database (NZGD).

2 CONSTRUCTION OF THE CBR CASE HISTORY DATABASE

The CBR case history database was populated using values of PGA, ground water table depth, and critical layer depths that were reported in Green et al. (2014) and using raw CPT data that was downloaded from the New Zealand Geotechnical Database (NZGD 2018). In the end, only 24 of the 25 sites from the Green et al. (2014) study were included in the CBR study because CPT data from one of the sites (Site 20) could not be located in the New Zealand Geotechnical Database. Of those 24 sites, 22 sites were included in the case history database and 2 sites were isolated to use as test cases.

The CPT data used in the CBR case history database only included raw values of depth, cone tip resistance q_c , cone side friction f_s , and pore pressure u_2 . The site-specific PGA values reported in Green et al. (2014) were originally estimated by the authors using conditional PGA distributions. These conditional PGA distributions were computed from accelograms recorded at strong motion stations throughout the region during the two earthquake events. The ground water table depths reported in Green et al. (2014) were estimated from the CPT data or P-wave refraction results. The identification of the critical layer depth range by the authors of Green et al. (2014) was aided by the use of soil behavior type index (I_c) and relative density (D_r) profiles derived from CPTs at each site. CPT-based liquefaction triggering procedures were used to identify the most critical layer only if there were credible alternative critical layers at a given site. From the authors of Green et al. (2014), the critical layer was defined as the following:

“In the context of this study, the “critical” layer is the soil layer that is believed to have liquefied and caused the observed surface manifestations for cases where surficial liquefaction manifestations were observed. For cases where no evidence of liquefaction was observed, the “critical” layer is that which is believed to be the most susceptible to liquefaction and that would have resulted in at least minor surficial manifestations if it indeed liquefied during an earthquake.”

In the CBR case history database, each case history is a discretized layer of a certain thickness with input parameters of depth, q_c , f_s , u_2 , PGA, and the binary occurrence of liquefaction triggering. The depth, q_c , f_s , and u_2 values were averaged over the depth range of the discretized layer, which for this study ranged from layer thicknesses of 0.05 to 0.20 m. As a result, a CPT sounding recorded in the depth range of 0.0 to 10.0 m that was discretized into 0.1-m thick layers would result in 100 case histories, each with a unique value of depth, q_c , f_s , and u_2 but with an identical values of PGA that corresponded to that site and specific earthquake event. The input parameter for liquefaction triggering was set as 0.0 if the depth of case history layer did not line up with the depth of the critical layer identified by Green et al. (2014) and was set to 1.0 if the two layers did line up. Layers that were located above the water table were removed from the case history database and from the set of test cases prior to the assessment so that only soils below the water table were evaluated for liquefaction triggering potential.

3 CBR FRAMEWORK FOR PREDICTION OF LIQUEFACTION TRIGGERING

In the framework of CBR, a case history database is composed of ‘old problems’ that will be matched to ‘new problems’ and of ‘old solutions’ that will be reused to solve ‘new problems’. Here the ‘old problems’ are defined as the combination of values of depth, q_c , f_s , u_2 , and PGA while the ‘old solution’ is whether or not liquefaction occurred. As such, the input parameters of the test cases that serve as ‘new problems’ to test the CBR case history database are also combinations of depth, q_c , f_s , u_2 , and PGA while the output, or ‘new solution’, will be whether or not liquefaction is predicted to occur based on the ‘old solutions’ from the most similar ‘old problems’.

The heart of the CBR method is the process of sorting the case history database to identify case histories that are most similar to the test case. The first step is to use parameter-specific similarity functions to compare an input parameter to all of the available parameters in the case study database. The result is a similarity index that ranks the each parameter in the case history database by how similar they are to the input test case parameter. The second step is

to weigh the similarity index of each parameter according to that parameter's relative importance to obtaining the overall solution. The final similarity score that is used to identify the case histories most similar to the test case is defined in Formula 1 and is the summation of the parameter-specific similarity index multiplied by the parameter-specific weight:

$$sim = sim_z \cdot w_z + sim_{qc} \cdot w_{qc} + sim_{fs} \cdot w_{fs} + sim_{u2} \cdot w_{u2} + sim_{PGA} \cdot w_{PGA} \quad (1)$$

where sim is the overall similarity score, $sim_{parameter}$ is the parameter-specific similarity index, and $w_{parameter}$ is the parameter-specific weight.

3.1 Similarity functions

The shape of the similarity functions used in this study were normalized normal probability density functions (PDFs). The shape of a normal PDF is defined by a mean value and a standard deviation, and the function was normalized so that it had a maximum value of 1.0 at the mean value. In this case, the standard deviation for the PDF-based similarity function of each parameter was defined as the standard deviation for that parameter in the subset of case histories that experienced liquefaction triggering. The standard deviations for each parameter from the subset of liquefied case histories are summarized in Table 1. The mean value for the PDF-based similarity function of each parameter was defined as the input value from a test case. As a result, the PDF-based similarity function for each parameter had a static value for the standard deviation but a unique mean value that varied according to the input from each test case. The similarity functions from Test Case #420 for the two parameters depth and f_s are shown in Figure 1. In Test Case #420, the input value for depth is 7.15 m and for f_s is 0.121 MPa, which were used as the mean values to define the PDF-based similarity functions. The standard deviations, which are not test case-dependent, were 2.13 m for the depth parameter and 0.02 MPa for the f_s parameter.

3.2 Weighting functions

The weighting functions for each parameter were evaluated using the statistical property coefficient of variation (C.O.V.) and were normalized so that the summation of the parameter weights was equal to 1.0. The C.O.V. of each parameter was evaluated once using the entire case history database and a second time using only the subset of case histories that experienced liquefaction. The non-normalized parameter weight was then defined as the ratio between the full database C.O.V.s and the liquefied database subset C.O.V. as shown in Formula 2. The weight was then normalized by dividing the parameter weight by the summation of all the parameter weights.

$$w_{parameter} = \frac{C.O.V._{parameter}\{All\ case\ histories\}}{C.O.V._{parameter}\{Liquefied\ case\ histories\}} \quad (2)$$

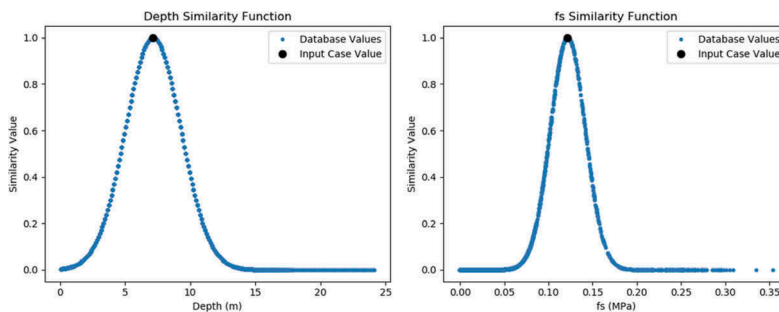


Figure 1. Similarity functions for the parameters a) depth and b) f_s as defined for the input Test Case #420. The black dot represents the input test case value and the blue dots are the values from the case history database.

Table 1. Summary of parameter-specific statistical characteristics used to define the shape of the PDFs for both the similarity functions and the parameter weights.

	Depth	q_c	f_s	u_2	PGA
Mean value for liquefied layers	5.01 m	5.72 MPa	0.03 MPa	0.03 MPa	0.27 g
Standard deviation for liquefied layers	2.13 m	2.61 MPa	0.02 MPa	0.03 MPa	0.10 g
C.O.V. for liquefied layers	0.42	0.46	0.58	1.19	0.36
Mean value for all layers	7.61 m	9.92 MPa	0.07 MPa	0.04 MPa	0.25 g
Standard deviation for all layers	4.67 m	7.37 MPa	0.07 MPa	0.05 MPa	0.09 g
C.O.V. for all layers	0.61	0.74	0.92	1.21	0.35
Normalized parameter weights	0.217	0.245	0.239	0.153	0.146

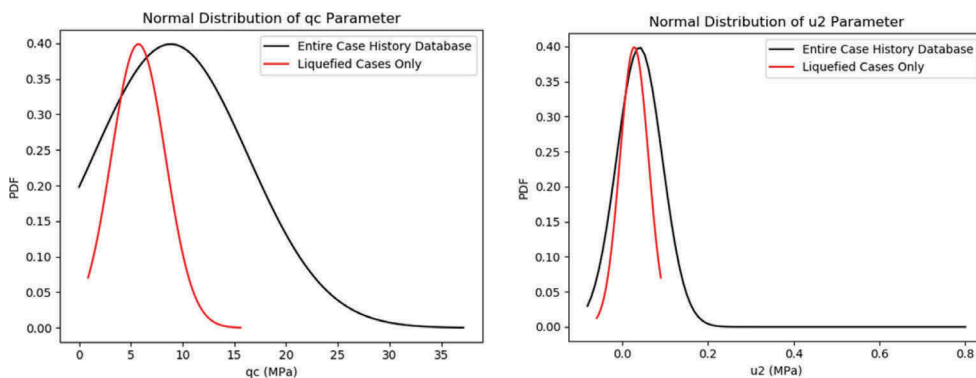


Figure 2. Normal PDFs of the a) q_c and b) u_2 parameters evaluated using the full case history database and the subset of case histories that experienced liquefaction.

This method of defining parameter weights reflects the recognition that parameters that are important to liquefaction triggering will likely have different statistical distributions than the parameters that are not important to liquefaction triggering. As seen in Figure 2a, the normal PDF of the q_c parameter defined using the full case history database is significantly different than the normal PDF defined using the subset of case histories that experienced liquefaction. In contrast, Figure 2b shows that there is little difference between the normal PDFs of the u_2 parameter defined using the full case history database and the subset of case histories that experienced liquefaction. The resulting weights, 0.251 for q_c and 0.151 for u_2 , reflect this presumed importance of each parameter based on differences between the full case history database and those case histories that experience liquefaction. Indeed, it makes sense that the q_c parameter has a much higher weight than the u_2 parameter for predicting liquefaction triggering. The full list of standard deviations, C.O.V.s, and weights for each of the parameters are summarized in Table 1.

4 RESULTS

Two of the 24 sites reviewed by Green et al. (2014) were set aside as test cases: Site 24 and Site 25. In addition to using the original identification of critical layers by the authors of Green et al. (2014) for a validation of the method, a second, independent analysis was performed for

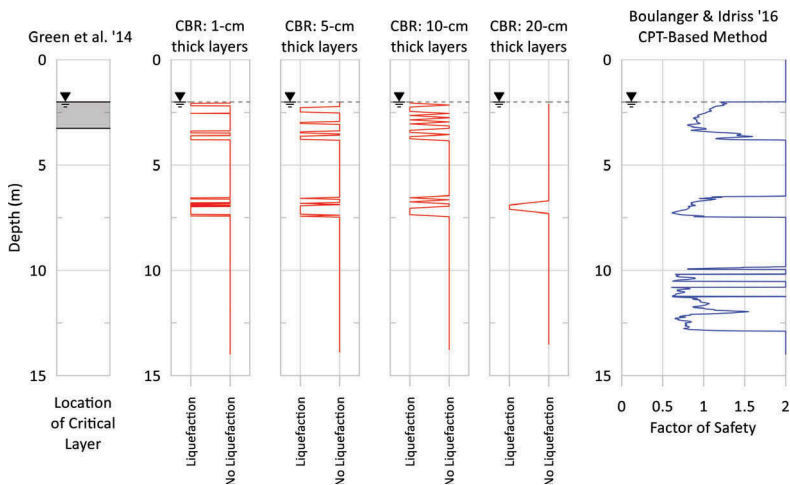


Figure 3. Location of the critical layer at Site 24 for the Darfield Earthquake (Mw 7.1, PGA 0.215 g) from Green et al. (2014) and predictions for liquefaction triggering from the CBR and Boulanger and Idriss (2016) methods.

comparison using the deterministic Boulanger and Idriss (2016) CPT-based method with a 15 % probability of liquefaction triggering. The analysis using the CBR method also included a simple sensitivity study to investigate the effect of layer discretization thickness on the results. In the sensitivity study, the four thicknesses used to discretize the site profiles into case histories and test cases were 1 cm, 5 cm, 10 cm, and 20 cm.

The results of the analysis using the three methods are presented in Figures 3 through 6. Figures 3 and 4 present the results for Site 24 as assessed for the Darfield Earthquake and the Christchurch Earthquake, respectively. Figures 5 and 6 present the results for Site 25 as assessed for the Darfield Earthquake and the Christchurch Earthquake, respectively.

At all four test sites, the CBR and Boulanger and Idriss (2016) methods accurately predicted the high liquefaction susceptibility of the critical layer that was identified by Green et al. (2014). It is further consistent with observations of surficial liquefaction reported in Green et al. (2014)

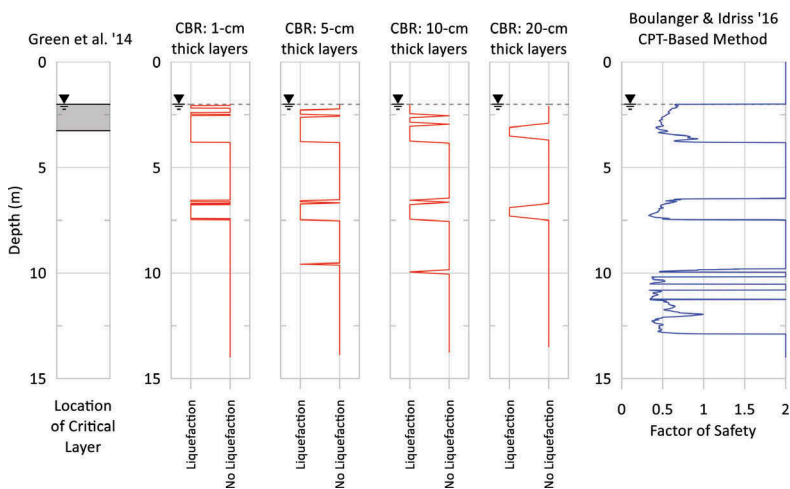


Figure 4. Location of the critical layer at Site 24 for the Christchurch Earthquake (Mw 6.2, PGA 0.450 g) from Green et al. (2014) and predictions for liquefaction triggering from the CBR and Boulanger and Idriss (2016) methods.

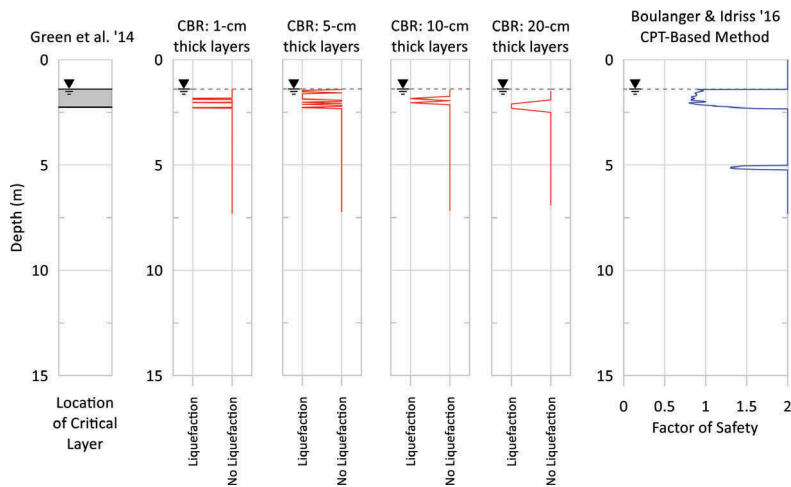


Figure 5. Location of the critical layer at Site 25 for the Darfield Earthquake (Mw 7.1, PGA 0.219 g) from Green et al. (2014) and predictions for liquefaction triggering from the CBR and Boulanger and Idriss (2016) methods.

that both the CBR and Idriss and Boulanger (2016) methods predicted larger levels of liquefaction triggering during the Christchurch Earthquake than during the Darfield Earthquake.

Using various layer discretization thicknesses with the CBR method had a small but observable effect on the accuracy of the results. In comparison to results from the Boulanger and Idriss (2016) method, the layer thicknesses 1 cm and 20 cm resulted in slightly worse, under predictions of liquefaction triggering than the 5 cm and 10 cm layer thicknesses. The method, however, is not particularly sensitive to the layer discretization thickness in this small range of values. The main observable difference between results from the CBR method and the Boulanger and Idriss (2016) method is that the CBR method consistently underestimates the amount of potential liquefaction triggering in comparison to the

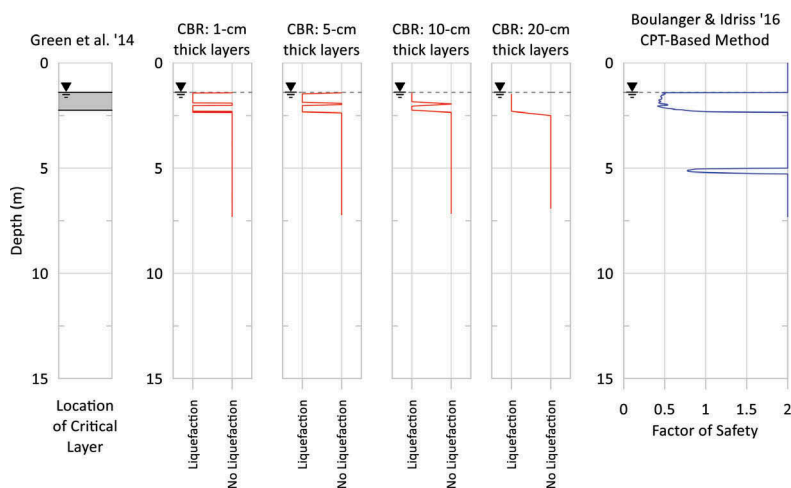


Figure 6. Location of the critical layer at Site 25 for the Christchurch Earthquake (Mw 6.2, PGA 0.453 g) from Green et al. (2014) and predictions for liquefaction triggering from the CBR and Boulanger and Idriss (2016) methods.

Boulanger and Idriss (2016) method. The main reason for the under prediction is the fact that the case history layers were only considered to have ‘liquefied’ if they lined up with the single most critical layer that was identified by Green et al. (2014). By this criterion, the case history database has mischaracterized the liquefaction triggering potential of other, frequently deeper layers that also could have liquefied during the same earthquake event. This shortcoming will be addressed in future work.

5 DISCUSSION AND CONCLUSIONS

In this study, CBR has been used successfully to predict liquefaction triggering at two test sites in Christchurch, New Zealand, under two different earthquake events. The CBR case history database was composed of data from 22 out of 24 available sites that were profiled by Green et al. (2014) and included raw CPT data (depth, q_c , f_s , and u_2), water table depths, site PGAs, and depth ranges of the critical layers. The raw CPT data was downloaded from the New Zealand Geotechnical Database and the water table depths, site PGAs, and critical layer depth ranges were sourced from Green et al. (2014). Each site was subjected to two separate earthquake events (the Darfield Earthquake and the Christchurch Earthquake), essentially doubling the number of cases in the case history database. A separate, independent assessment of liquefaction triggering potential was performed at each test site for comparison using the deterministic Boulanger and Idriss (2016) CPT-based method with a 15% probability of liquefaction triggering.

At three out of the four test cases, the CBR method and the Boulanger and Idriss (2016) methods correctly predicted liquefaction triggering of the critical layer that was identified by Green et al. (2014). At the fourth site, Site 24 during the Darfield Earthquake, both the CBR and the Boulanger and Idriss (2016) methods also predicted the liquefaction triggering of the critical layer that was identified by Green et al. (2014), but this site had no observable manifestations of liquefaction triggering from the Darfield Earthquake.

A simple sensitivity study to assess the effect of layer discretization thickness showed that the results of CBR are not particularly sensitive to selected case history layer thicknesses in the range of 1 cm to 20 cm, but higher accuracy in comparison to the Boulanger and Idriss (2016) method was seen with layer thicknesses of 5 cm and 10 cm.

The objective of this study is not to replace widely used CPT-based methods for liquefaction triggering assessment, but rather to serve as a proof of concept for the use of CBR in geotechnical engineering applications. The future goal of this work would be to move beyond predictions of liquefaction triggering and into more important applications such as the direct prediction of liquefaction severity and the consequences of liquefaction triggering that include settlement, lateral spreading, and structural damage. The current procedure for evaluating many of these consequences involves stringing together several empirical methods that each address one aspect of soil liquefaction. It is hoped that in the future, CBR can take advantage of the large body of case histories from around the world that have been and continue to be well-documented by researchers, and to create a unified, method-free approach for predicting the consequences of liquefaction triggering.

ACKNOWLEDGEMENTS

The authors would like to thank Amir Kaynia and Brian Carlton of NGI for their discussions and advice around the implementation of CBR for soil liquefaction prediction applications and Kerstin Bach of NTNU for her valuable support in bringing CBR into geotechnical engineering (Engin et al. 2018). The authors would also like to acknowledge the New Zealand Geotechnical Database for the CPT data used in this study as well as the authors of Green et al. (2014) for contributing 25 high-quality liquefaction case histories to the geotechnical earthquake engineering community.

REFERENCES

- Aamodt, A. and Plaza, E. 1994. Case-Based Reasoning: Foundational Issues, Methodological Variations, and System Approaches. *AI Communications*. IOS Press, Vol. 7: 1, pp. 39-59.
- Boulanger, R. W., and Idriss, I. M. 2016. CPT-Based Liquefaction Triggering Procedure. *J. of Geotechnical and Geoenvironmental Engineering*. Vol. 142(2): 04015065.
- Engin, H. K., Nadim, F., Carotenuto, P. and Bach, K. 2018. Estimation of pile capacities using Case Base Reasoning method. *4th Int. Symposium on Computational Geomechanics, 2-4 May, 2018, Assisi, Italy*.
- Garcia de Soto, B. and Adey, B. T. 2015. Investigation of the case-based reasoning retrieval process to estimate resources in construction projects. *Creative Construction Conference 2015*. Procedia Engineering Vol. 123, pp. 169-181.
- Goh, Y. M. and Chua, K. H. 2009. Case-Based Reasoning for Construction Hazard Identification: Case Representation and Retrieval. *J. of Construction Eng. and Management*. Vol. 135(11): pp. 1181-1189.
- Green, R. A., Cubrinovski, M., Cox, B., Wood, C., Wotherspoon, L., Bradley, B., and Maurer, B. 2014. Select Liquefaction Case Histories from the 2010-2011 Canterbury Earthquake Sequence. *Earthquake Spectra*. Vol. 30, No. 1, pp. 131-153.
- Juwaied, N. S. 2018. Applications of Artificial Intelligence in Geotechnical Engineering. *ARPJ Journal of Engineering and Applied Sciences*. Vol. 13, No. 8, pp. 2764-2785.
- Kim, S. and Shim, J. H. 2014. Combining case-based reasoning with genetic algorithm optimization for preliminary cost estimation in construction industry. *Canadian Journal of Civil Eng.* Vol. 41, pp. 65-73.
- Kolodner, J.L. 1992. An Introduction to Case-Based Reasoning. *Art. Intelligence Review*. Vol. 6, pp. 3-34.
- Lesniak, A. and Zima, K. 2018. Cost Calculation of Construction Projects Including Sustainability Factors Using the Case Based Reasoning (CBR) Method. *Sustainability*. Vol. 10(5): 1608.
- NZGD (2016). New Zealand Geotechnical Database. <<https://www.nzgd.org.nz>>. New Zealand Earthquake Commission (EQC). Accessed 5 June 2018.
- Rankin, J. H., Froese, T. M., and Waugh, L. M. 1999. Exploring the Application of Case-Based Reasoning to Computer-Assisted Construction Planning. *Proceedings of Durability of Building Materials and Components 8*. pp. 2526-2536.
- Ryu, H., Lee, H., and Park, M. 2007. Construction Planning Method Using Case-Based Reasoning (CONPLA-CBR). *Journal of Computing in Civil Engineering*. Vol. 21(6): pp. 410-422.
- Yau, N. and Yang, J. 1996. A Case-Based Reasoning Approach for Construction Planning. *Proceedings of the 13th International Symposium on Automation and Robotics in Construction*. Tokyo. 11-13 June.
- Yoon, Y., Jung, J., and Hyun C. 2016. Decision-making Support Systems Using Case-based Reasoning for Construction Project Delivery Method Selection: Focused on the Road Construction Projects in Korea. *The Open Civil Engineering Journal*. Vol. 10: pp. 500-512.
- Zima, K. 2015. The Case-Based Reasoning Model Of Cost Estimation At The Preliminary Stage Of A Construction Project. *ORSDCE Colloquium*. Procedia Engineering. Vol. 122: pp. 57-64.